Metabolism of 4-*n*-Nonylphenol by Non-modified and CYP1A1- and CYP1A2-Transgenic Cell Cultures of Tobacco

Angelika Berger, Alexander S. Ruß, Ingolf Schuphan, and Burkhard Schmidt*

Institute of Biology V, Chair: Ecology/Ecotoxicology/Ecochemistry, RWTH Aachen University, Worringerweg 1, D-52056 Aachen, Germany. Fax: +49-241-8022182.
E-mail: burkhard.schmidt@post.rwth-aachen.de

* Author for correspondence and reprint requests

Z. Naturforsch. **60 c**, 883–892 (2005); received August 1/31, 2005

The metabolism of ^{14}C-4-*n*-nonylphenol (^{14}C-4-*n*-NP), as a model for the xenoestrogen nonylphenol, was investigated in three types of tobacco cell suspension cultures: one genetically non-modified culture (NT) and two cultures constitutively expressing human cytochrome P450 CYP1A1 or CYP1A2. With 1 mg l^{-1} of ^{14}C-4-*n*-NP and 24 h of incubation, the xenobiotic was transformed almost completely to glycosides. After glycosidic cleavage, ^{14}C-4-*n*-NP and several primary metabolites of ^{14}C-4-*n*-NP were liberated. Portions of the primary metabolites were 29.3% (NT culture), 34.3% (CYP1A1 culture), and 50.7% of applied ^{14}C (CYP1A2 culture). Thus, the endogenous capacity of the tobacco cells to form primary metabolites of 4-*n*-NP was noticeably higher than that of CYP1A1 or CYP1A2. The results however clearly suggest that 4-*n*-NP is – even though a poor – substrate of CYP1A1 and CYP1A2. In order to examine metabolic profiles of 4-*n*-NP in the NT, CYP1A1 and CYP1A2 cultures, the suspensions were exposed to 10 mg l^{-1} of ^{14}C-4-*n*-NP using a two-liquid-phase system with carrier *n*-hexadecane and 192 h of incubation. Results obtained resembled those of the low concentration study. The oxidative metabolic profiles determined after hydrolytic cleavage using GC-EIMS were similar in the NT, CYP1A1 and CYP1A2 cultures. Main metabolites were side-chain mono-hydroxylated derivatives of 4-*n*-NP with 6′-, 7′- and 8′-OH-4-*n*-NP as prominent metabolites. In addition, olefinic side-chain hydroxy, ring methoxylated, keto and ring hydroxylated derivatives were observed. The lack of differences in metabolic profiles among the CYP1A1, CYP1A2 and NT cultures was referred to the low enzymatic activity of CYP1A1 and CYP1A2 as compared to the higher endogenous oxidative capacity of tobacco, as well as to similar metabolic profiles of 4-*n*-NP produced by CYP1A1 and CYP1A2 and tobacco itself.

Key words: 4-*n*-Nonylphenol, Oxidative Metabolic Profiling, Transgenic Plant Cell Culture

Introduction

In recent years, valuable information on substrate specificities of P450 isozymes concerning xenobiotics was derived from studies using bacteria (*e.g.* Parikh *et al.*, 1997) or yeasts (*e.g.* Inui *et al.*, 2001) heterologously expressing the corresponding genes. Both expression systems show no or only low endogenous P450 activity. In addition, commercially available microsomes containing selected (human) P450 species are utilized, which are derived from the baculovirus expression system. All systems mentioned so far, however, require the co-expression of NADPH-P450 reductase in order to obtain catalytically active P450s. Overexpression of mammalian P450 isozymes in higher plants, *e.g.* tobacco and potato, was shown to enhance the oxidative metabolism of *e.g.* herbicides (Inui *et al.*, 2000, 2001; Inui and Ohkawa 2005). In these experiments, co-expression of mammalian NADPH-P450 reductase was not necessary, since the foreign P450s were supplied with the requisite electrons by endogenous plant reductases. Recently, we similarly produced transgenic cell suspension cultures of tobacco overexpressing human P450 CYP1A1 or CYP1A2 (each under control of a constituitive promotor). These P450-transgenic *in vitro* systems were subsequently used to examine successfully the metabolism of atrazine and metamitron. In addition to metabolic pathways, it was shown that the main oxidized metabolites of both herbicides could be generated in 100–200 μg amounts per cell culture assay (Bode, 2004; Bode *et al.*, 2004).

In the present investigation, this conception of 'oxidative metabolic profiling' is applied to the xenoestrogen (endocrine disruptor) nonylphenol,

0939–5075/2005/1100–0883 $ 06.00

which emerges prevailingly in the environment or in foodstuffs as degradation product of nonylphenol polyethoxylates; these are used world-wide as *e.g.* detergents and emulsifiers (Thiele *et al.*, 1997; Staples *et al.*, 1999; Guenther *et al.*, 2002). Industrially produced nonylphenol contains about 90% of 4-nonylphenol, which consists of a mixture of branched-chain (C_9) isomers (Wheeler *et al.*, 1997; Nakagawa *et al.*, 2004; Ruß *et al.* 2005). Though straight-chain 4-*n*-nonylphenol is rather not a component of industrially produced nonylphenol, a number of metabolism studies was performed with this model compound, *e.g.* in plant tissues (Bokern *et al.*, 1996; Schmidt and Schuphan, 2002; Schmidt *et al.*, 2003, 2004). The relevance of experiments with 4-*n*-nonylphenol is discussed – especially concerning endocrine and toxic effects. However, we could demonstrate that in *Agrostemma githago* plant cell suspension cultures, similar metabolites were formed from straight-chain 4-*n*-nonylphenol (Schmidt *et al.*, 2003) and branched-chain 4-(3′,5′-dimethyl-3′-heptyl)-phenol (Schmidt *et al.*, 2004), which is a prominent component of the industrial mixture (Ruß *et al.*, 2005). The main metabolites formed by *A. githago* from both isomers were glycosides of the parent itself and of several side-chain hydroxylated (primary) metabolites. Part of the studies were executed in a two-liquid-phase system using *n*-hexadecane (0.5%, v/v) as carrier for application of higher amounts of the highly lipophilic nonylphenol isomers. On the whole, these findings make 4-*n*-nonylphenol an attractive nonylphenol model compound for the present metabolism studies with the CYP1A1- and CYP1A2-transgenic cell cultures of tobacco.

The objectives of the present investigation were to examine whether (i) 4-*n*-nonylphenol is biotransformed by non-modified tobacco cell suspension cultures (including metabolic profile), (ii) 4-*n*-nonylphenol is substrate of human CYP1A1 or CYP1A2 expressed in tobacco cell suspension cultures (including metabolic profile), and (iii) the concept of 'oxidative metabolic profiling' using P450-transgenic tobacco cell cultures can be applied to 4-*n*-nonylphenol. In order to obtain higher amounts of the metabolites, part of the studies were performed in a two-liquid-phase system described previously (Schmidt *et al.*, 2003).

Materials and Methods

Chemicals

[*Ring*-U-^{14}C]-4-*n*-nonylphenol (^{14}C-4-*n*-NP; specific activity: 1,080.4 MBq mmol $^{-1}$; radiochemical purity: > 98% due to HPLC analysis) was supplied by Hartmann Analytic (Braunschweig, Germany). Non-labelled 4-*n*-nonylphenol was provided by Promochem (Wesel, Germany). For the metabolism studies, the specific activity of the radiochemical was adjusted to 833 Bq μg^{-1} (183.3 MBq mmol^{-1}; 20 μg assays) or 150 Bq μg^{-1} (33.0 MBq mmol^{-1}; 200 μg assays).

Cell cultures and treatments

The P450-transgenic cultures (CYP1A1, CYP1A2) were produced from the corresponding non-transformed tobacco cell suspension cultures (*Nicotiana tabacum* L.; NT), which were provided by DSMZ (Braunschweig, Germany). Stable genetic transformation and cultivation of the cultures utilized for the studies were described (Bode, 2004; Bode *et al.*, 2004). The cultivation cycle of all cultures was 10 d; cultivation and metabolism studies were executed in 100 ml Erlenmeyer flasks. In the first study (20 μg assays), the cell suspensions were treated with 20 μg (1×10^6 dpm, in 20 μl methanol) of ^{14}C-4-*n*-NP per assay 9 d after subcultivation, and were then incubated for 24 h. Cultures of the second study (200 μg assays) were treated with 200 μg (1.8×10^6 dpm, in 100 μl *n*-hexadecane) of ^{14}C-4-*n*-NP per assay; *n*-hexadecane constituted the organic phase of the two-liquid-phase system. These assays were then incubated for 192 h. The studies were executed using 2 (20 μg assays) or 3 parallels (200 μg assays).

Extraction procedures and initial analysis

Concerning the 20 μg assays, media were separated from cells by suction filtration and analyzed by liquid scintillation counting (LSC; LS 6500 analyzer, Beckman, Munich, Germany). The cells were stored in chloroform/methanol (1:2, v/v) at – 20 °C for 16 h and were extracted with this solvent mixture by means of sonication (Bandelin, Berlin, Germany). Insoluble cell debris were separated by suction filtration and washed with chloroform/methanol/water (1:2:0.8 v/v/v). Portions of ^{14}C contained in extracts were examined by LSC. Insoluble cell debris were air-dried and subjected to combustion analysis (Biological Oxidizer OX

500; Zinsser Instruments, Frankfurt, Germany) for the determination of non-extractable residues.

Concerning the 200 μg assays, entire assays were transferred to centrifuge tubes, and 10 ml of hexane were added in order to separate the *n*-hexadecane phases. After centrifugation (15 min, 5,000 × *g*), organic phases were removed and subjected to LSC. Remaining media and cells were treated as described before (20 μg assays). The individual media and cell extracts were analyzed by TLC.

Hydrolysis procedure

Hydrolysis was performed using a mixture of 2 M HCl and methanol (1:1 v/v) for 2 h at reflux (Markham, 1982). The methanol portion of the reaction mixture was then removed and the remaining aqueous phase was extracted with diethyl ether. Portions of ^{14}C found in extracts (designated as hydrolysates) and those in the aqueous phases were determined by LSC.

Chromatographic procedures

Analytic thin-layer chromatography (TLC) was performed on silica gel plates SIL G-25 UV_{254} (0.25 mm) supplied by Macherey-Nagel (Düren, Germany). Solvent systems were A: *n*-hexane/diethyl ether/acetic acid 50:50:1 (v/v/v), B: ethyl acetate/iso-propanol 40:60 (v/v), C: ethyl acetate/iso-propanol/water 64:24:4 (v/v/v), and D: *n*-hexane/diethyl ether/acetic acid 20:80:1 (v/v/v). Occasionally, TLC plates were developed using systems A, B and C, successively. Separated ^{14}C spots were located and quantified using a Tracemaster 40 radiochromatogram scanner (Berthold, Wildbad, Germany); non-labelled 4-*n*-NP was detected under UV light at 254 nm.

High-performance liquid chromatography (HPLC) was performed on a Beckman System Gold Personal chromatograph (München, Germany) consisting of Programmable Solvent Module 126 and Diode Array Detector Modul 168. This system was connected to a Ramona 5 radiodetector equipped with a 1655 quartz cell (glass, 32–45 μm; internal diameter: 4.0 mm; cell volume: 0.4 ml) supplied by Raytest (Straubenhardt, Germany). All HPLC analyses were performed at 20 °C on a reversed phase column (CC 250/4 Nucleosil 100–5 C18 HD; Macherey-Nagel, Düren, Germany) using a flow of 1 ml min^{-1}. Non-labelled 4-*n*-NP was detected at 280 nm. Elution was carried out with solvents A (0.1% acetic acid in water) and B (0.1% acetic acid in acetonitrile) as follows: A/B 65:35 (v/v) for 5 min, linear 30 min gradient to 100% B, isocratic B (100%) for 5 min, and return to initial conditions within 5 min. All HPLC analyses were performed with an injection volume of 100 μl and terminated by washing the column for 5 min with the initial solvent system. For isolation of metabolite fractions, same conditions were used with repeated collection of fractions at the outlet of the system.

GC-EIMS was performed using a Hewlett-Packard 5890 Series II gas chromatograph (Agilent Technologies, Waldbronn, Germany) equipped with a FS-SE-54-NB-0.5 column (25 m × 0.25 mm, 0.46 μm film thickness; CS Chromatographie Service, Langerwehe, Germany). The gas chromatograph was connected to a Hewlett-Packard 5971 A MSD (mass selective detector), which was operated in the scan mode (mass range *m/z* 50–500) with an electron energy of 70 eV. Carrier gas was helium, and injection volume was 1 μl.

Derivatization

Samples were derivatized with 100 μl of *N*-methyl-*N*-trimethylsilyltrifluoroacetamide (MSTFA; Fluka, Buchs, Switzerland) at 70 °C for 30 min in closed crimp cap vials. Reaction mixtures were directly injected into the GC-EIMS apparatus. Acetylation of samples was performed with 1 ml acetic acid anhydride and 1 ml pyridine overnight. Then, the anhydride and the solvent were removed under reduced pressure, and the remaining residue was dissolved in methanol for GC-EIMS injection. Derivatization with trimethyl orthoacetate was executed as follows: Samples were dissolved in 0.4 ml acetic acid anhydride, 0.1 ml acetic acid and 2 ml of trimethyl orthoacetate, and were heated to 105 °C for 4 h. Then, the solvent was removed, and the remaining residue was dissolved in methanol.

Results and Discussion

Distribution of radioactivity

Concerning the 20 μg assays (data not shown), the majority of ^{14}C was present in cell extracts (79.9–86.4% of applied radioactivity), while portions below 10% were detected in both, the media and cell debris. The recovered radioactivity was above 95% with all assays, which suggests that transformation of ^{14}C-4-*n*-NP to $^{14}CO_2$ and volatile organics, or volatilization of parent ^{14}C-4-*n*-NP

Table I. Distributions of radioactivity in non-transformed (NT) and P450-transgenic (CYP1A1 and CYP1A2) tobacco cell suspension cultures after application of 200 μg of ^{14}C-4-*n*-nonylphenol at the end of the incubation interval: 3 parallels, 1,800,000 dpm per assay (applied in 100 μl of *n*-hexadecane), 192 h of incubation. Data are averages of parallels, excepting portions of primary metabolites, and are given as % of applied ^{14}C.

	NT	CYP1A1	CYP1A2
Media	21.6	21.8	34.8
Hexadecane phases	7.3	10.1	12.4
Cell extracts	48.2	58.8	41.2
Non-extractable ^{14}C	14.8	2.6	3.2
Recovered ^{14}C	91.9	93.3	91.6
Primary metabolites[a]	32.6	44.0	22.5

[a] According to HPLC analysis of hydrolysates (extracts of hydrolysis experiments).

from the flasks was negligible. Individual analyses with TLC (systems A and D) demonstrated that in the media and cell extracts of the 20 μg assays, free ^{14}C-4-*n*-NP was present only in minor amounts (non-transformed tobacco cultures, NT: 4.4%; *cyp1a1*-transformed cultures, CYP1A1: 12.6%) or completely absent (*cyp1a2*-transformed cultures, CYP1A2). The chromatographic behaviour of ^{14}C contained in all cell extracts with systems A–D pointed to glycosides as metabolic products.

Regarding the 200 μg assays of the two-liquid-phase study (Table I), 21.6–34.8% of applied ^{14}C were detected in media and 41.2–58.8% in cell extracts. Remaining portions were associated with cell debris (2.6–14.8%) or *n*-hexandecane phases. While recoveries of ^{14}C were above 90%, free ^{14}C-4-*n*-NP was found in none of the 200 μg assays. As with the 20 μg assays, the radioactivity in the cell extracts appeared to consist of glycosides (TLC solvent systems B and C). With all TLC systems used, the radioactivity in the media proved to be immobile. Extraction of these ^{14}C portions with organic solvents was not successful; the same held true for hydrolysis procedures in order to cleave possible glycosidic or ester linkages. HPLC analysis was not practicable, since the necessary concentration of the media resulted in highly viscous samples.

Concerning distribution of ^{14}C, the results obtained with the non-modified and P450-transgenic tobacco cells were comparable to data published recently on the biotransformation of 4-*n*-NP and the branched-chain isomer 4-(3′,5′-dimethyl-3′-heptyl)-phenol by *Agrostemma githago* cells – also using the same two-liquid-phase system (Schmidt *et al.*, 2003, 2004). Uptake of 4-*n*-NP from the *n*-hexadecane layer by the tobbacco cells was considered satisfactory. The same held for recoveries of ^{14}C, noticeable portions of soluble ^{14}C in the cell extracts and complete disappearance (turnover) of applied 4-*n*-NP. Generally, the formation of glycosides from the phenolic xenobiotic or its possible primary transformation products was expected according to data published on nonylphenol (Bokern *et al.*, 1996; Schmidt and Schuphan, 2002; Schmidt *et al.*, 2003, 2004). The chemical nature of the radioactivity present in the media remained obscure. Recently, ^{14}C materials with similar behaviour were found in media after application of 4-(3′,5′-dimethyl-3′-heptyl)-phenol and suspected to consist of polymerized or co-polymerized products of the isomer (Schmidt *et al.*, 2004).

Hydrolysis of conjugates and isolation of primary 4-n-NP metabolites

The cell extracts of parallels were combined and subjected to hydrolysis (2 M HCl/methanol, reflux), in order to release the expected ^{14}C-aglycons from their corresponding glycosides. With both, the 20 and 200 μg assays, almost 100% of the radioactivity introduced in the hydrolysis experiments was recovered in the corresponding hydrolysates (diethyl ether extracts of reaction mixtures). Minor losses were observed after concentration. All hydrolysates were examined using TLC (systems A and D) and HPLC. The results of HPLC analysis demonstrated (Fig. 1; samples derived from 200 μg assays) that similar peak patterns (R_t 15–30 min) were obtained from the NT, CYP1A1 and CYP1A2 cultures. All peaks were preponderantly absent before hydrolysis; thus the corresponding compounds were liberated from their glycosides by acid treatment.

The peak with R_t 26–29 min (fraction 3) was traced back to the parent by cochromatography with authentic ^{14}C-4-*n*-NP. Its area percentages were: NT, 64.5% (20 μg) and 32.2% (200 μg); CYP1A1, 57.0% (20 μg) and 25.2% (200 μg); CYP1A2, 38.4% (20 μg) and 45.5% (200 μg). The second group of peaks appeared at R_t 21–25 min (fraction 2); percentages were: NT, 18.3% (20 μg) and 47.2% (200 μg); CYP1A1, 24.7% (20 μg) and 43.4% (200 μg); CYP1A2, 42.6% (20 μg) and

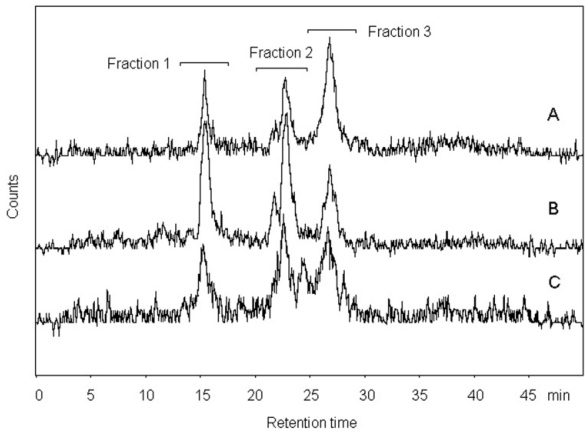

Fig. 1. HPLC radiochromatograms of the hydrolysates (cell extracts) obtained from non-transformed (A), and CYP1A1- (B) and CYP1A2-transgenic (C) tobacco cell suspension cultures (data of 200 μg experiment are displayed); fractions 1–3 were isolated for GC-EIMS analysis.

32.2% (200 μg). Another peak group was observed at R_t 15–18 min (fraction 1): NT, 15.8% (20 μg) and 20.5% (200 μg); CYP1A1, 18.2% (20 μg) and 31.5% (200 μg); CYP1A2, 16.1% (20 μg) and 22.4% (200 μg). Fractions 1 and 2 were regarded as primary metabolites of ^{14}C-4-*n*-NP. In the hydrolysates derived from the 200 μg assays, corresponding portions were prevailingly higher (as compared to the 20 μg assays) with a maximum value of about 75% in case of the CYP1A1 culture. Based on applied radioactivity however, percentages of primary metabolites were lower in the 200 μg assays (Table I) due to lower ^{14}C portions detected in the cell extracts. This fact may be referred to the extended incubation interval (24 h *vs.* 192 h) and consequently further biotransformation steps with regard to applied ^{14}C-4-*n*-NP. Nevertheless, total amounts of primary metabolites (fractions 1 and 2) produced by the NT, CYP1A1 and CYP1A2 cultures were about 60 μg, 80 μg and 40 μg per 200 μg assay, respectively. The radioactivity contained in the hydrolysates of the 200 μg assays was separated using multiple HPLC runs for fraction 1 (R_t 15–18 min), 2 (R_t 21–25 min) and 3 (R_t 26–29 min).

Identification of 4-n-NP metabolites by GC-EIMS

According to previously published data on 4-*n*-NP and a 4-NP isomer (Schmidt *et al.*, 2003, 2004), the isolated HPLC fractions 1 and 3 were reacted with MSTFA to trimethylsilyl derivatives. These were examined by GC-EIMS. In fractions 1 isolated from both, the genetically non-modified and the two P450-transgenic tobacco cultures, 13 peaks (I to XIII) were detected (Fig. 2A), which could be traced back to 4-*n*-NP. Due to their mass spectra, peaks I to V were identified by the side-chain hydroxylated products 4′-OH-4-*n*-NP to 8′-OH-4-*n*-NP (Table II). A thorough dicussion of these mass spectra was published recently (Schmidt *et al.*, 2003). Prominent fragments were *m/z* 290 resulting from cleavage of $HOSi(CH_3)_3$ (with subsequent degradation of side-chain), *m/z* 173 (I), 159 (II), 145 (III), 131 (IV) or 117 (V) derived from the fragments $(CH_3)_3SiOCHR^{+\bullet}$ (with R = CH_3 to C_5H_{11}, indicating the position of side-chain OH), and *m/z* 179 derived from fragment $(CH_3)_3SiOC_6H_4CH_2^{+\bullet}$.

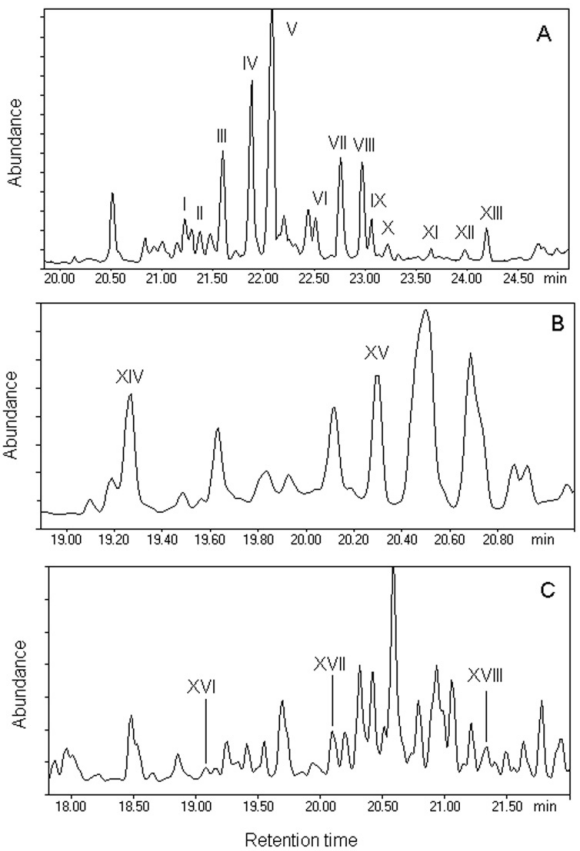

Fig. 2. GC-EIMS chromatograms (after trimethylsilyl derivatization) of fractions 1 (A; 1A1 culture shown), 2 (C; 1A1 culture shown) and 3 (B; NT culture shown) obtained from the hydrolysates (cell extracts) by HPLC isolation.

Table II. EI mass spectra (trimethylsilyl derivatives) and portions of 4-*n*-nonylphenol (4-*n*-NP) and its metabolites observed in HPLC fractions 1 (R_t 15–18 min) and 3 (R_t 26–29 min), which were derived from the hydrolysates of the non-transformed (NT) and P450-transgenic (CYP1A1, CYP1A2) tobacco cell suspension cultures. Abundance of mass spectral fragments was determined from data of CYP1A1 culture; percentages were based on peak area; total area of peaks detected in the fraction corresponds with 100%.

GC-MS peak: R_t [min]	EIMS *m/z* (abundance in %)	Compound[a]	NT portion (%)	CYP1A1 portion (%)	CYP1A2 portion (%)
HPLC fraction 1					
I: 21.24	380 (1, M^+), 365 (1), 290 (1), 253 (1), 219 (11), 205 (2), 192 (100), 179 (9), 173 (7), 73 (31)	4′-OH-4-*n*-NP	4.0	3.9	3.0
II: 21.38	380 (1, M^+), 365 (1), 290 (22), 261 (1), 253 (1), 233 (13), 205 (28), 192 (23), 179 (31), 159 (19), 147 (5), 73 (100)	5′-OH-4-*n*-NP	3.2	3.0	3.3
III: 21.61	380 (2, M^+), 365 (1), 337 (2), 290 (25), 247 (5), 219 (1), 205 (39), 192 (10), 179 (61), 163 (4), 145 (53), 73 (100)	6′-OH-4-*n*-NP	14.3	10.2	13.8
IV: 21.89	380 (5, M^+), 365 (2), 351 (6), 290 (21), 261 (2), 253 (3), 219 (3), 205 (23), 192 (8), 179 (75), 163 (3), 131 (92), 73 (100)	7′-OH-4-*n*-NP	19.4	19.1	20.5
V: 22.09	380 (6, M^+), 365 (2), 290 (11), 253 (6), 219 (1), 205 (12), 192 (5), 179 (70), 163 (3), 117 (100), 73 (72)	8′-OH-4-*n*-NP	26.6	26.8	30.5
VI: 22.52	378 (2, M^+), 363 (1), 335 (1), 288 (6), 245 (10), 218 (59), 205 (6), 179 (33), 171 (21), 145 (15), 75 (33), 73 (100)	6′-OH-4-*n*-NenP[b]	4.9	4.4	3.5
VII: 22.76	378 (1, M^+), 363 (1), 288 (6), 259 (9), 231 (6), 217 (5), 205 (10), 192 (86), 179 (40), 157 (21), 131 (22), 73 (100)	7′-OH-4-*n*-NenP[b]	9.7	10.4	8.5
VIII: 22.98	378 (2, M^+), 363 (2), 288 (3), 231 (11), 217 (8), 205 (19), 192 (96), 179 (17), 143 (22), 117 (58), 73 (100)	8′-OH-4-*n*-NenP[b]	8.7	9.5	8.0
IX: 23.06	410 (9, M^+), 395 (1), 381 (3), 320 (3), 290 (1), 235 (5), 209 (38), 193 (4), 179 (37), 131 (56), 73 (100)	7′-OH-*ring*-OCH_3-4-*n*-NP[b]	3.6	3.9	4.3
X: 23.23	410 (10, M^+), 395 (1), 353 (3), 320 (1), 235 (1), 209 (43), 193 (4), 179 (43), 117 (70), 73 (100)	8′-OH-*ring*-OCH_3-4-*n*-NP[b]	1.4	2.2	sh[c]
XI: 23.65	378 (7, M^+), 363 (1), 288 (1), 245 (6), 231 (5), 217 (4), 205 (54), 192 (20), 179 (17), 147 (7), 129 (7), 115 (11), 103 (10), 73 (100)	9′-OH-4-*n*-NenP[b]	1.2	1.6	1.7
XII: 23.98	408 (4, M^+), 393 (1), 379 (19), 318 (3), 289 (5), 264 (4), 247 (5), 235 (4), 222 (28), 209 (25), 192 (8), 179 (7), 157 (20), 131 (27), 73 (100)	7′-OH-*ring*-OCH_3-4-*n*-NenP[b]	1.0	1.8	1.5
XIII: 24.20	408 (1, M^+), 393 (1), 384 (2), 369 (12), 247 (3), 235 (3), 222 (7), 209 (3), 179 (3), 145 (30), 117 (95), 73 (100)	8′-OH-*ring*-OCH_3-4-*n*-NenP[b]	1.1	3.2	1.4
HPLC fraction 3					
XIV: 19.27	292 (13 , M^+), 277 (2), 192 (1), 179 (100), 149 (3), 117 (1), 91 (4), 73 (35)	4-*n*-NP	100	49.0	46.0
XV: 20.30	290 (28 , M^+), 275 (4), 256 (1), 205 (100), 192 (14), 189 (24), 179 (28), 163 (5), 149 (4), 129 (4), 115 (18), 91 (4), 73 (63)	4-*n*-NenP[b]	sh[c]	51.0	54.0

[a] Structures of 4-*n*-nonylphenol metabolites are proposed according to EIMS fragmentation patterns: 4′-OH-4-*n*-NP to 8′-OH-4-*n*-NP: side-chain hydroxylated derivatives of 4-*n*-NP; 6′-OH-4-*n*-NenP to 9′-OH-4-*n*-NenP: side-chain hydroxylated olefinic derivatives of 4-*n*-NP; 7′-OH-*ring*-OCH_3-4-*n*-NP and 8′-OH-*ring*-OCH_3-4-*n*-NP: side-chain hydroxylated and ring methoxylated derivatives of 4-*n*-NP; 7′-OH-*ring*-OCH_3-4-*n*-NenP and 8′-OH-*ring*-OCH_3-4-*n*-NenP: side-chain hydroxylated and ring methoxylated olefinic derivatives of 4-*n*-NP; 4-*n*-NeP: olefinic derivative of 4-*n*-NP.

[b] Position of double bond in nonenyl derivatives (NenP) and position of OCH_3 substitution of the aromatic ring could not be identified.

[c] Detected as shoulder; integration was not possible.

Similarily, peaks VI, VII, VIII and XI were regarded as signals of side-chain hydroxylated olefinic metabolites 6′-OH-4-*n*-NenP to 9′-OH-4-*n*-NenP. The double bonds appeared to be located between the respective side-chain OH function and the aromatic ring, though exact positions remained unclear. The same holds for their origin. Both, enzymatic catalysis in the cells or chemical reactions, *e.g.* during hydrolysis (HCl/methanol at reflux), may have lead to formation of alkenes most probably from intermediary doubly hydroxylated products. The mass spectral fragmentation of 6′-OH-4-*n*-NenP was interpreted as follows (values are *m/z*): 378, $M^{+\bullet}$; 363, $-CH_3$; 335, $-C_3H_7$; 288, $-HOSi(CH_3)_3$; 245, $288-C_3H_7$; 218, $245-C_2H_3$; 179, $(CH_3)_3SiOC_6H_4CH_2^{+\bullet}$; 145 $(CH_3)_3SiOCHC_3H_7^{+\bullet}$ (indicator of position of OH); 75, $HO=Si(CH_3)_2^{+\bullet}$; 73, $Si(CH_3)_3^{+\bullet}$. Characteristic fragments of 7′-OH-4-*n*-NenP, 8′-OH-4-*n*-NenP and 9′-OH-4-*n*-NenP, respectively, were *m/z* 131, $(CH_3)_3SiOCHC_2H_5^{+\bullet}$; 117, $(CH_3)_3SiOCHCH_3^{+\bullet}$; and 103, $(CH_3)_3SiOCH_2^{+\bullet}$ (positions of OH).

Peaks IX and X were identified by 7′-OH-*ring*-OCH_3-4-*n*-NP and 8′-OH-*ring*-OCH_3-4-*n*-NP. The positions of OCH_3 (*ortho* or *meta* to phenolic function) remained unknown, whereas the fragmentation patterns unequivocally proved that substitution was on the ring; 7′-OH-*ring*-OCH_3-4-*n*-NP (*m/z*): 410, $M^{+\bullet}$; 395, $-CH_3$; 381, $-C_2H_5$; 320, $-HOSi(CH_3)_3$; 290, $320-OCH_2$; 209, $(CH_3)_3SiOC_6H_4(OCH_3)CH_2^{+\bullet}$ (proof of ring substitution); 179, $209-OCH_3$; 131, $(CH_3)_3SiOCHC_2H_5^{+\bullet}$; 73, $Si(CH_3)_3^{+\bullet}$. A similar mass spectrum was obtained for 8′-OH-*ring*-OCH_3-4-*n*-NP with *m/z* 117, $(CH_3)_3SiOCHCH_3^{+\bullet}$ indicating the position of side-chain OH. According to analogous argumentation, peaks XII and XIII were regarded as signals of 7′-OH-*ring*-OCH_3-4-*n*-NenP and 8′-OH-*ring*-OCH_3-4-*n*-NenP.

With HPLC fraction 3, two 4-*n*-NP derived peaks were observed (Fig. 2B; Table: II) in all three tobacco cell cultures examined: parent 4-*n*-NP itself (XIV) and olefinic 4-*n*-NenP (XV). The mass spectrum of 4-*n*-NP derived from the metabolism experiments corresponded with that of an authentic reference (both as trimethylsily derivatives). 4-*n*-NenP's mass spectrum was similar to that of parent 4-*n*-NP – however with base peak at *m/z* 205 (as compared to *m/z* 179 in case of 4-*n*-NP). This fact may indicate that the olefinic bond was located between C-2′ and C-3′ of the side-chain.

Since transformation products of ^{14}C-4-*n*-NP corresponding with fraction 2 were not detected in previous studies using several plant cell cultures (Schmidt *et al.*, 2003; Schmidt and Schuphan, 2002), different derivatization strategies were employed in order to examine these fractions by GC-EIMS. Due to similar chromatographic behaviour during HPLC and TLC (discussed later), it was assumed that roughly similar products were contained in fractions 2 obtained from the NT, CYP1A1 and CYP1A2 cultures. Fraction 2 resulting from NT cultures was trimethylsilyl derivatized (MSTFA). In the GC-EIMS chromatogram (Fig. 2C), three peaks (XVI–XVIII) were identified which were traced back to applied ^{14}C-4-*n*-NP (Table III). Metabolic product XVI was tentatively identified by *ring*-OH-4-*n*-NP (XVI). Besides *m/z* 380 ($M^{+\bullet}$), 365 ($-CH_3$) and 323 ($-C_4H_9$), main support for ring substitution in XVI came from fragment *m/z* 267, resulting from $[(CH_3)_3SiO]_2C_6H_3CH_2^{+\bullet}$ ($-C_8H_{17}$), and absence of *m/z* 290 (see discussion before). Fragment *m/z* 305 was thought to result from $(CH_3)_3SiOC_6H_3(C_9H_{19})CH_2^{+\bullet}$ after cleavage of $HOSi(CH_2)_2$). Compound XVII's mass spectrum with apparent $M^{+\bullet}$ at *m/z* 306 pointed to keto-4-*n*-NP, though not all MS peaks could be referred unequivocally to defined fragments. The base peak at *m/z* 209 seemed to originate from $(CH_3)_3SiOC_6H_4CH(OH)CH_2^{+\bullet}$ after succesive cleavage of alkyl groups (*m/z* 291, 249); fragments with *m/z* 195 and 179 were attributed to $209-CH_2$ and $209-CH_2O$, respectively. Similarly, trace metabolite XVIII possibly was keto-*ring*-OCH_3-4-*n*-NP with $M^{+\bullet}$ at *m/z* 336. The proposed chemical structures XVI–XVIII were also reasonable regarding their HPLC elution between fraction 3 (less polar) and 1 (more polar).

Fraction 2 derived from the CYP1A1 culture was acetylated. In the GC-EIMS chromatogram, one peak was detected which was related to ^{14}C-4-*n*-NP (Table III). Due to its $M^{+\bullet}$ at *m/z* 276, the compound was identified by the acetate of keto-4-*n*-NP. Further characteristic peaks appeared at *m/z* 234 ($-COCH_2$), 179 ($234-C_4H_7$), 137 ($179-C_3H_6$), and 123 ($137-CH_2$). The latter two fragments corresponded with *m/z* 209 and 195, respectively, of the trimethylsily derivatized sample (NT cultures). In fraction 2 (reacted with trimethyl orthoacetate) obtained from the CYP1A2 culture, only 4-*n*-NP was found either free or as acetate (Table III). Their mass spectra agreed with those of authentic

Table III. EI mass spectra (derivatives as indicated below) and portions of 4-*n*-nonylphenol (4-*n*-NP) and its metabolites observed in HPLC fraction 2 (R_t 21–25 min) derived from the hydrolysates of the non-transformed (NT) and P450-transgenic (CYP1A1, CYP1A2) tobacco cell suspension cultures. Portions were based on peak area; total area of peaks detected in the fraction corresponds with 100%.

GC-MS peak: R_t [min]	EIMS *m/z* (abundance in %)	Compound[a]	NT portion (%)	CYP1A1 portion (%)	CYP1A2 portion (%)
Trimethyl silyl derivatized					
XVI: 19.09	380 (3, M^+), 365 (1), 323 (4), 305 (50), 267 (9), 225 (3), 216 (2), 179 (6), 147 (18), 103 (7), 73 (100)	*Ring*-OH-4-*n*-NP[b]	25.0	–[c]	–[c]
XVII: 20.10	306 (26, M^+), 291 (4), 249 (16), 209 (100), 195 (54), 179 (67), 166 (19), 159 (15), 151 (23), 117 (10), 73 (66)	Keto-4-*n*-NP[b]	75.0	–[c]	–[c]
XVIII: 21.36	336 (5, M^+), 321 (1), 306 (1), 283 (10), 209 (8), 194 (5), 147 (10), 131 (93), 117 (8), 73 (100)	Keto-*ring*-OCH_3-4-*n*-NP[b]	tr[d]	–[c]	–[c]
Acetyl derivatized					
XIX: 20.58	276 (3, M^+), 234 (35), 219 (10), 217 (11), 179 (56), 163 (10), 148 (14), 137 (100), 133 (31), 123 (95), 107 (29)	Keto-4-*n*-NP acetate[b]	–[c]	100	–[c]
Trimethyl orthoacetate derivatized					
XX: 18.74	220 (8, M^+), 107 (100), 77 (5)	4-*n*-NP, underivatized	–[c]	–[c]	58.7
XXI: 19.75	262 (1, M^+), 220 (29), 107 (100), 77 (5)	4-*n*-NP acetate	–[c]	–[c]	41.3

[a] Structures of 4-*n*-nonylphenol metabolites are proposed according to EIMS fragmentation patterns: *Ring*-OH-4-*n*-NP: ring hydroxylated derivative of 4-*n*-NP; Keto-4-*n*-NP: side-chain keto derivative of 4-*n*-NP; Keto-*ring*-OCH_3-4-*n*-NP: side-chain keto and ring methoxylated derivative of 4-*n*-NP.
[b] Position of carbonyl group of keto derivatives, and position of OCH_3 and additional OH substitution of the aromatic ring could not be identified.
[c] Not performed.
[d] Detected as trace; integration was not possible.

samples. It was supposed that 4-*n*-NP was a contamination of fraction 2 due to a slight overlap of HPLC fractions 2 and 3. Although three transformation products could be identified in HPLC fraction 2, total peak areas were too small to account for entire amounts of ^{14}C present in samples. In addition, fraction 2 showed an unexpected and undefined behaviour by TLC as compared to that observed by HPLC. Most of the radioactivity of fraction 2 was immobile with solvents A, B and D. So, the compounds identified in fractions 2 with GC-EIMS were thought to represent only a part of the metabolites present. Instability of compounds XVI–XVIII during TLC (but stability by HPLC) was rather excluded.

Metabolism of 4-n-NP in non-modified, CYP1A1- and CYP1A2-transgenic tobacco cell suspensions

In the P450-transgenic (CYP1A1, CYP1A2) and non-modified (NT) tobacco cell cultures, 4-*n*-NP was metabolized to a comparable extent. This finding contrasts with previous studies using atrazine and metamitron, where both herbicides were transformed extremely more rapidly by the CYP1A1 or CYP1A2 cultures than by the corresponding NT culture (Bode, 2004; Bode *et al.*, 2004). Partly, this lack of difference can be attributed to glycosylation, which is an important metabolic pathway with phenolic 4-*n*-NP. Nevertheless, the question arises, whether 4-*n*-NP is substrate of human CYP1A1 or CYP1A2. Evaluation of the data obtained by HPLC analysis of the hydrolysates (of the cell extracts) revealed that in case of

the 20 μg experiment, a total of 29.3% of primary metabolites were detected in the NT, 34.3% in the CYP1A1, and 50.7% in the CYP1A2 culture (values based on applied ^{14}C). These data were supported by results of TLC analysis. Taking into account the unidentified products contained in media and the non-extractable ^{14}C, which both may have been formed from primary metabolites, differences become even more distinct (HPLC: 41.0%, 51.3% and 66.0%, respectively). These results prove that 4-*n*-NP is metabolized to a higher extent to primary metabolites by the CYP1A1 and CYP1A2 cultures as compared to the NT culture. The endogenous capacity of the tobacco cells to form primary metabolites of the xenobiotic, however, appears to be noticeably higher than that of CYP1A1 or CYP1A2. According to corresponding data of the 200 μg assays, only culture CYP1A1 demonstrated a higher turnover than the NT culture. On the whole, the results of the 200 μg experiment were not as clear-cut as those from the 20 μg experiment; this ambiguous finding was referred to the rather artificial two-liquid-phase system and longer incubation interval utilized in this study. Using recombinant yeast microsomes expressing human P450 isozymes, Inui *et al.* (2001) found that 4-*n*-NP was substrate of CYP1A2 (besides CYP2B6 and CYP2C19) but not of CYP1A1. Involvement of P450s in the metabolism of (branched-chain) 4-nonylphenol was concluded from *in vivo* and *in vitro* studies with rainbow trout (Mehldahl *et al.*, 1996) and pond snails (Lalah *et al.*, 2003a, b). Lee *et al.* (1998) studied the transformation of three branched-chain isomers in rat and human microsomes. By means of specific inducers and inhibitors, the authors demonstrated that CYP2B isozymes (of both, rats and humans), especially CYP2B2, are predominant in nonylphenol metabolism. Due to results published by Lee *et al.* (1996a, b), nonylphenol may be substrate of rat hepatic CYP1A and CYP3A isozymes, whereas data reported by Mehldahl *et al.* (1996) indicated that rainbow trout CYP1A1 is not responsible for nonylphenol biotransformation. The present results partly agree with these – inconsistent – literature data; our results clearly suggest that 4-*n*-NP is transformed by CYP1A1 and CYP1A2; the xenobiotic, however, seems to be a poor substrate of both P450s.

The metabolic profiles of 4-*n*-NP metabolism in the CYP1A1, CYP1A2 and NT cultures were determined by GC-EIMS analysis of HPLC fraction 1–3, which were derived from the 200 μg assays. Concentrations of metabolites were too low in order to perform a thorough analysis with corresponding fractions from the 20 μg experiment. The data proved that the primary 4-*n*-NP metabolites identified with HPLC and TLC analysis were unequivocally produced by oxidative reactions, and that similar profiles were obtained from the CYP1A1, CYP1A2 and NT cultures. In all cell cultures studied, the main metabolites detected in fraction 1 were side-chain mono-hydroxylated derivatives of 4-*n*-NP with 6′-, 7′- and 8′-OH-4-*n*-NP as main products. This finding mainly agrees with data published previously on the metabolism of nonylphenol in plant tissues (Bokern *et al.*, 1996; Bokern und Harms, 1997; Schmidt and Schuphan, 2002; Schmidt *et al.*, 2003, 2004). Besides olefinic hydroxy derivatives described before (Bokern *et al.*, 1996; Schmidt *et al.*, 2003), ring methoxylated derivatives were detected, which were thought to originate from the hydroxylated precursors. The lack of distinct differences among the CYP1A1, CYP1A2 and NT cultures concerning the metabolic profile of 4-*n*-NP may be due to the low enzymatic activity of CYP1A1 and CYP1A2 towards 4-*n*-NP, which was possibly covered by endogenous oxidative capacities of the tobacco cells. It is additionally conceivable that CYP1A1 and CYP1A2 produced similar 4-*n*-NP metabolic profiles as the tobacco suspension itself (*i.e.* culture NT). Mehldahl *et al.* (1996) reported that several nonylphenol isomers were transformed to side-chain hydroxy derivatives by rainbow trout. Similar products were suspected from studies with rat and human hepatic microsomes (Lee *et al.*, 1998). In trout, 4-*n*-NP was shown to be metabolized to ring or side-chain hydroxylated metabolites (Coldham *et al.*, 1998), while Inui *et al.* (2001) similarly demonstrated that human CYP1A2 expressed in yeast microsomes transformed the compound to ring or side-chain hydroxylated derivatives. Lalah *et al.* (2003a, b) found a catechol derivative of a branched-chain nonylphenol isomer after exposure to pond snails. A glucuronide of a catechol derivative was also reported by Doerge *et al.* (2002) following administration of nonylphenol to rats.

Acknowledgements

The authors wish to thank Mrs. H. Patti and Mrs. B. Thiede for technical assistance, Prof. Dr. F. P. Guengerich (Vanderbilt University School of

Medicine, Nashville, Tennessee, USA) for providing cDNA of human CYP1A1 and CYP1A2, and the Aachen Graduate College: Elimination of Endocrine-Disrupting Chemicals from Waste Water (AGEESA; funded by Deutsche Forschungsgemeinschaft DFG) for ^{14}C-4-*n*-nonylphenol.

Bode M. (2004), Studien zum Metabolismus von Pestiziden und Xenobiotika durch humane Cytochrom P450-Monooxygenasen in transgenen Tabakzellkulturen. Thesis, RWTH Aachen University.

Bode M., Stöbe P., Thiede B., Schuphan I., and Schmidt B. (2004), Biotransformation of atrazine in transgenic tobacco cell culture expressing human P450. Pest Manag. Sci. **60**, 49–58.

Bokern M. and Harms H. (1997), Toxicity and metabolism of 4-*n*-nonylphenol in cell suspension cultures of different plant species. Environ. Toxicol. Chem. **31**, 1849–1854.

Bokern M., Nimtz M., and Harms H. (1996), Metabolites of 4-*n*-nonylphenol in wheat cell suspension cultures. J. Agric. Food Chem. **44**, 1123–1127.

Coldham N. G., Sivapathasundaram S. D. M., Ashfield L. A., and Pottinger T. G. (1998), Biotransformation, tissue distribution, and persistence of 4-nonylphenol residues in juvenile rainbow trout (*Oncorhynchus mykiss*). Drug Metab. Dispos. **26**, 347–354.

Doerge D. R., Twaddle N. C., Churchwell M. I., Chang H. C., Newbold R. R., and Delclos K. B. (2002), Mass spectrometric determination of *p*-nonylphenol metabolism and disposition following oral administration to Sprague-Dawley rats. Reprod. Toxicol. **16**, 45–56.

Guenther K., Heinke V., Thiele B., Kleist E., Prast A., and Raecker T. (2002), Endocrine disrupting nonylphenols are ubiquitous in food. Environ. Sci. Technol. **36**, 1676–1680.

Inui H. and Ohkawa H. (2005), Herbicide resistance in transgenic plants with mammalian P450 monooxygenase genes. Pest. Manag. Sci. **61**, 286–291.

Inui H., Kodama T., Ohkawa Y., and Ohkawa H. (2000), Herbicide metabolism and cross-tolerance in transgenic potato plants co-expressing human CYP1A1, CYP2B6 and CYP2C19. Pestic. Biochem. Physiol. **66**, 116–129.

Inui H., Shiota N., Motoi Y., Ido Y., Inoue T., Kodama T., Ohkawa Y., and Ohkawa H. (2001), Metabolism of herbicides and other chemicals in human cytochrome P450 species and in transgenic potato plants co-expressing human CYP1A1, CYP2B6 and CYP2C19. J. Pestic. Sci. **26**, 28–40.

Lalah J. O., Schramm K.-W., Severin G. F., Lenoir D., Henkelmann B., Behechti A., Guenther K., and Kettrup A. (2003a), *In vivo* metabolism and organ distribution of a branched ^{14}C-nonylphenol isomer in pond snails, *Lymnaea stagnalis* L. Aquat. Toxicol. **62**, 305–319.

Lalah J. O., Behechti A., Severin G. F., Lenoir D., Guenther K., Kettrup A., and Schramm K.-W. (2003b), The bioaccumulation and fate of a branched ^{14}C-*p*-nonylphenol isomer in *Lymnaea stagnalis* L. Environ. Toxicol. Chem. **22**, 1428–1436.

Lee P. C., Chakraborty-Patra C., Stelloh C. T., Lee W., and Struve M. (1996a), Interaction of nonylphenol and hepatic CYP1A in rats. Biochem. Pharmacol. **27**, 885–889.

Lee P. C., Chakraborty-Patra S., and Struve M. (1996b), Modulation of rat hepatic CYP3A by nonylphenol. Xenobiotica **26**, 831–838.

Lee P. C., Marquardt M., and Lech J. J. (1998), Metabolism of nonylphenol by rat and human microsomes. Toxicol. Lett. **99**, 117–126.

Markham K. R. (1982), Techniques of Flavonoid Identification. Academic Press, London.

Mehldahl A. C., Nithipatikom K., and Lech J. J. (1996), Metabolism of several ^{14}C-nonylphenol isomers in rainbow trout (*Oncorhynchus mykiss*): *in vivo* and *in vitro* microsomal metabolites. Xenobiotica **26**, 1167–1180.

Nakagawa T., Sugaya N., Sakurai K., Nakagawa J., Usukura K., Onda N., and Oguma K. (2004), Simultaneous detection of endocrine disruptors of 4-nonyl phenols and 4-octyl phenols in commodity products using positive chemical ionization-gas chromatography/mass spectrometry. Chromatographia **25**, 25–32.

Parikh A., Gillam E. M. J., and Guengerich F. P. (1997), Drug metabolism by *Escherichia coli* expressing human cytochromes P450. Nature Biotechnol. **15**, 784–788.

Ruß A. S., Vinken R., Schuphan I., and Schmidt B. (2005), Synthesis of branched *para*-nonylphenol isomers: Occurrence and quantification in two commercial mixtures. Chemosphere **60**, 1624–1635.

Schmidt B. and Schuphan I. (2002), Metabolism of the xenooestrogens 4-*n*-nonylphenol and bisphenol A in plant cell suspension cultures. In: Book of Abstracts, Vol. 2, 10th IUPAC International Congress on the Chemistry of Crop Protection, Basel, August 4–9. IUPAC, Basel, p. 34.

Schmidt B., Patti H., Niewersch C., and Schuphan I. (2003), Metabolism of [*ring*-U-^{14}C]-4-*n*-nonylphenol by *Agrostemma githago* cell culture in a two-liquid-phase system. Biotechnol. Lett. **25**, 1375–1381.

Schmidt B., Patti H., Hommes G., and Schuphan I. (2004), Metabolism of the nonylphenol isomer [*ring*-U-^{14}C]-4-(3′,5′-dimethyl-3′-heptyl)-phenol by cell suspension cultures of *Agrostemma githago* and soybean. J. Environ. Sci. Health B **39**, 533–549.

Staples C. A., Williams J. B., Blessing R. J., and Varineau P. T. (1999), Measuring the biodegradability of nonylphenol ether carboxylates, octylphenol ether carboxylates, and nonylphenol. Chemosphere **38**, 2029–2039.

Thiele B., Günther K., and Schwuger M. J. (1997), Alkylphenol ethoxylates: trace analysis and environmental behaviour. Chem. Rev. **97**, 3247–3272.

Wheeler T. F., Heim J. R., LaTorre M. R., and Janes A. B. (1997), Mass spectral characterization of *p*-nonylphenol isomers using high-resolution capillary GC-MS. J. Chromatogr. Sci. **35**, 19–30.